Quantitative Symmetry and Chirality of the Molecular Building Blocks of Quartz

ARTICLE *in* CHEMISTRY OF MATERIALS · DECEMBER 2002

Impact Factor: 8.35 · DOI: 10.1021/cm0207806

2 AUTHORS:

Dina Einot-Yogev
The Open University of Israel
5 PUBLICATIONS **57** CITATIONS
SEE PROFILE

David Avnir
Hebrew University of Jerusalem
384 PUBLICATIONS **16,730** CITATIONS
SEE PROFILE

Quantitative Symmetry and Chirality of the Molecular Building Blocks of Quartz

Dina Yogev-Einot and David Avnir*

Institute of Chemistry and The Lise Meitner Minerva Center for Computational Quantum Chemistry, The Hebrew University of Jerusalem, Jerusalem 91904, Israel

Received July 25, 2002. Revised Manuscript Received October 23, 2002

We introduce the use of the concept of continuity in symmetry and chirality as a novel descriptor of the structure of the building blocks of materials. These measures are of global nature, and take into account all angles and bond lengths of the molecular building blocks. The particular example we have selected for a detailed analysis is (low) quartz. All of its main building blocks, namely the elementary SiO_4 tetrahedron, the $Si(OSi)_4$ unit, the silicon atoms tetrahedron $SiSi_4$, and six of its internal helical structures, were investigated in detail as to their degree of chirality, tetrahedricity content, degree of distortion from C_2-symmetry, and more. Specific chirality is defined and its value determined for low and high quartz and for cristobalite. The most chiral unit within quartz was found to be a four-SiO_4 segment helix.

1. Background: General Motivation for This Study

Many material properties are inherently associated with the symmetry of the building block (its point group) and with its packing symmetry (the space group). Whereas the treatment of symmetry/material-property relations has been carried out mainly in terms of exact symmetry groups, quite often these symmetries are only approximate. These imperfect symmetries can be found from the molecular level (the molecular building blocks of materials), through mesoscopic scales (small aggregates and clusters, liquid crystals), and up to macroscopic objects. There is therefore a current problem which is quite major: exact symmetry language and tools are used for the treatment of common cases where symmetry is, at most, only nearly exact. Let us exemplify the symmetry problem with a specific example that will serve us also later on, namely the SiO_4 unit.

The SiO_4 tetrahedron is a common molecular building block of thousands of materials. These include some 900 natural silicates,[1] many natural[2] and synthetic[3] zeolites (such as the intensively studied MCM materials[4]), numerous noncrystalline solids including various glasses, a vast range of porous materials,[5] composites prepared by the sol−gel process[6] and many more. It is evident therefore that the SiO_4 unit is a very versatile "Lego-type" building block, with which one can construct practically endless types of different structures, both crystalline and disordered. What makes it so versatile? It turns out that while the SiO_4 unit is fairly rigid and nearly tetrahedral (deviations from perfect tetrahedral symmetry were first noticed by Jones and Taylor in feldspars silicate[7] and a year later in quartz[8,9]), the $Si(OM)_4$ unit (where M is Si, Al, etc.) is the one which displays a rich variety of combinations of Si−O−M bond angles (from 180° down to 120° [1]), of tilt angles between neighboring tetrahedral units, and of bond lengths.[10] Thus, while the first shell tetrahedron, SiO_4, retains much of its tetrahedricity, the second shell tetrahedron, SiM_4, may (but need not) be distorted. Traditionally, these distortions of silicon-oxide based materials have been investigated − both experimentally and theoretically − in terms of specific geometric parameters such as bond angles and bond lengths, which are obtained from either X-ray data analyses or from theoretical calculations.[11,12] However, this specific-parameter approach has suffered from a basic difficulty. First, in the vast majority of the crystalline and noncrystalline silicon oxide-based materials, the Si−O−M and the O−Si−O bond angles need not distort uniquely, but each of the angles may distort differently; and second, the distortion of the molecular building block shows up not only in its angles but also in the bond lengths, all four of which may, again, need not be equal. Approaches to treat this inherent difficulty have been in several directions. One approach has been to use averages of the main distortive parameters, such as taking an average of angles;[10,13,14] another has been to display

* To whom correspondence should be addressed. E-mail: david@chem.ch.huji.ac.il.

(1) Liebau, F. *Structural Chemistry of Silicates*; Springer-Verlag: Berlin/Heidelberg, 1985.
(2) Szostak, R. *Molecular Sieves*; Blackie Academic & Professional: London, 1998.
(3) *http://www.iza-structure.org/databases/* Structure Commission (12A), 2001.
(4) Raman, N. K.; Anderson, M. T.; Brinker, C. J. *Chem. Mater.* **1996**, *8* (8), 1682.
(5) Nakanishi, K. *J. Porous Mater.* **1997**, *4* (2), 67.
(6) Schubert, U.; Kickelbick, G.; Husing, N. *Mol. Cryst. Liq. Cryst.* **2000**, *354*, 695.
(7) Jones, J. B.; Taylor, W. H. *Acta Crystallogr.* **1961**, *14*, 443.
(8) Young, R. A.; Post, B. *Acta Crystallogr.* **1962**, *15*, 337.
(9) Smith, G. S.; Alexander, L. E. *Acta Crystallogr.* **1963**, *16*, 462.
(10) Robinson, K.; Gibbs, G. V.; Ribbe, P. H. *Science* **1971**, *172*, 567.
(11) Gibbs, G. V.; Boisen, M. B., Jr. In *The Chemistry of Organic Silicon Compounds*; Rappoport, Z., Apeloig, Y., Eds.; Wiley & Sons: Chichester, U. K., 1998; Vol. 2, chapter 2, p 103.
(12) Wright, A. C. *J. Non-Cryst. Solids* **1994**, *179*, 84.
(13) Grimm, H.; Dorner, B. *J. Phys. Chem. Solids* **1975**, *36*, 407.

10.1021/cm0207806 CCC: $25.00
Published on Web 12/24/2002

separately each of the relevant geometric parameters and their changes;[15] and a third has been even to assume that distorted structural features are actually not distorted (such as the assumption that the SiO_4 unit is a perfect tetrahedron[16]). We propose, therefore, that what is crucially needed in materials science is a *global view* of the overall distortion, which takes into account *all* of the specific changes in a unified form.

How then is it possible to look at the distortion of a structure as a global whole which takes into account simultaneously all angles and bond-lengths? A structural feature of the building blocks, which indeed provides such a global view is their *symmetry*. For instance, the various SiO_2-based materials do differ in their "degree of tetrahedricity"[17] (to be defined shortly), and even more so the second shell tetrahedron, $SiSi_4$ (of the $Si(OSi)_4$ unit). Hence, if one could indeed measure *the degree of symmetry on a quantitative continuous level*, then one would have at hand a new structure-analysis tool that would relate to the whole, and would open the possibility of searching for correlations with properties which are inherently dependent on symmetry.

The quantitative measurements of symmetry and of chirality have been a major theme of research and development in our research group, and in Section 2 we briefly overview its main elements, which are needed for this report. In fact, this report is the first in which we extend the now well-developed symmetry-measurement methodology to the world of materials science, and we have selected quartz for that purpose. Why quartz?

We made this selection because of the unique structural properties of this material which we list in Section 3; because it is a classical prototype of the large family of SiO_2-based materials; and because it is a first step toward the understanding of symmetry and chirality issues of *disordered* SiO_2 materials in general, and sol−gel materials in particular.[18,19] One of many questions associated with sol−gel materials in this context is, for instance, what makes the molecular building blocks of sol−gel materials suitable for (chiral) templating.[18,20]

The most dominant structural characteristic of quartz is the overall arrangement of the SiO_4 tetrahedra in a beautiful double-helix (Figure 1, left) leading to its chirality. The question of the local origin of long-range structural features is one of the more interesting ones in materials science, and we shall return to it in detail below. The chirality of quartz leads to some important properties: quartz rotates polarized light (the first material recognized with this property[21−24]), and it is piezoelectric.[25] Before entering the detailed symmetry and chirality analysis of the molecular building blocks of quartz, we outline the methodology of the measurement of symmetry and chirality and introduce the concept of specific symmetry and specific chirality.

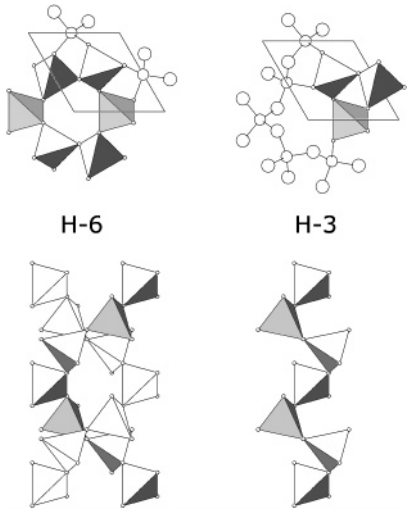

Figure 1. Molecular helical structure of low quartz ($P3_221$). Top: Projection along **c** axis. Bottom: Side view along the **b** axis. Helix H-3 (right) has three SiO_4 tetrahedra per turn. Helix H-6 has six tetrahedra per turn. H-6 is composed of a pair of helices of the same handedness, one of which is shown (bottom left) with shadows, and the other without shadows.

2. Quantitative Evaluation of the Degree of Symmetry and Degree of Chirality

2.1. General Overview. We have developed the notion that it is natural to evaluate, on a quantitative scale, how much of a given symmetry there is in a structure.[26−28] Toward the implementation of this notion we developed a general symmetry measurement tool which is based on finding the minimal distances that the points of a shape have to undergo in order for it to attain the desired symmetry. It is a special distance function in that the target shape itself is unknown a priori. Using this measurement procedure − the continuous symmetry measure (CSM) − it has become possible to evaluate quantitatively how much of any symmetry exists in a nonsymmetric configuration; what is the nearest symmetry to that configuration; and what is the actual shape of the nearest symmetric structure. Closely related is the continuous chirality measure (CCM) which evaluates the distance to the nearest achiral symmetry point group.[29] We have demonstrated the feasibility and versatility of this approach on a wide variety of symmetry/chirality related issues. Examples include the measurement of the symmetry content of distorted classical polyhedra;[30−32] the assessment of the

(14) Lager, G. A.; Jorgensen, J. D.; Rotella, F. J. *J. Appl. Phys.* **1982**, *53* (10), 6751.
(15) D'Amour, H.; Denner, W.; Schulz, H. *Acta Crystallogr.* **1979**, *B35*, 550.
(16) Silvi, B.; D'Arco, Ph.; Saunders, V. R.; Dovesi, R. *Phys. Chem. Miner.* **1991**, *17*, 674.
(17) Zabrodsky, H.; Peleg, S.; Avnir, D. *J. Am. Chem. Soc.* **1993**, *115*, 8278 (Erratum: 11, 656).
(18) Marx, S.; Liron, Z. *Chem. Mater.* **2001**, *13* (10), 3624.
(19) Moreau, J. J. E.; Vellutini, L.; Man, M. W. C.; Bied, C. *J. Am. Chem. Soc* **2001**, *123* (7), 1509.
(20) Srebnik, S.; Lev, O.; Avnir, D. *Chem. Mater.* **2001**, *13*, 811.
(21) Bio't, J. B. *Me'm Inst.* **1812**, *1*, 1−372.
(22) Applequist, J. *Am. Sci.* **1987**, *75*, 59.
(23) Schurig, V. *Enantiomer* **1997**, *2*, 135.
(24) Kauffman, G. B.; Bernal, I.; Schutt, H.-W. *Enantiomer* **1999**, *4*, 33.
(25) Heising, R. A. *Quartz Crystals for Electrical Circuits*; D. Van Nostrand Company, Inc.: New York, 1947.
(26) Avnir, D.; Zabrodsky Hel-Or, H.; Mezey, P. G. In *Encyclopedia of Computational Chemistry*; von Rague Schleyer, P., Ed.; Wiley: Chichester, U. K., 1998; Vol. 4.
(27) Avnir, D.; Katzenelson, O.; Keinan, S.; Pinsky, M.; Pinto, Y.; Salomon, Y.; Zabrodsky Hel-Or, H. In *Concepts in Chemistry: A Contemporary Challenge*; Rouvray, D. H., Ed.; Research Studies Press Ltd: Taunton, England, 1997; Chapter 9.
(28) Zabrodsky, H.; Peleg, S.; Avnir, D. *J. Am. Chem. Soc.* **1992**, *114*, 7843.
(29) Zabrodsky, H.; Avnir, D. *J. Am. Chem. Soc.* **1995**, *117*, 462.

symmetry content of objects which contain an element of randomness in their construction;[33] symmetry analyses of small clusters[34] and of large disordered aggregates;[35] symmetry and chirality analyses of enzymatic activities, establishing quantitative symmetry as a novel tool in QSAR studies;[36,37] and the identification of many correlations between symmetry/chirality and molecular properties, examples being correlations between spectral properties and the degree of symmetry distortion[38] and a correlation between the degree of the chirality and the efficiency of chromatographic chiral separation.[39] In general, it became clear from these studies and from studies of other research groups[31,40−48] that the global-shape descriptors − quantitative symmetry and quantitative chirality − shed new light on many classical problems in structural chemistry.

2.2. CSM and CCM Methodologies. *I. Degree of Symmetry.* According to the CSM methodology,[17,28] given a (distorted) structure composed of N vertexes, the coordinates of which are $\{Q_k\ ,\ k = 1,2...N\}$, one searches for the vertex coordinates of the nearest perfectly G-symmetric object (G being a specific symmetry group), $\{P_k = 1,2...N\}$. Once at hand, the symmetry measure is defined as

$$S(G) = 100 \times \min \frac{1}{N \times D^2} \sum_{k=1}^{N} |Q_k - P_k|^2 = 100 \times \min \frac{\sum_{k=1}^{N} |Q_k - P_k|^2}{\sum_{k=1}^{N} |Q_k - Q_0|^2} \quad (1)$$

where Q_0 is the coordinates vector of the center of mass of the investigated structure, and where the denominator is a mean square size normalization factor, D, summing over all N distances from Q_0 to the vertexes of the original structure. It was proven elsewhere[28] that the bounds are $100 \leq S \leq 0$: if a structure has the desired G-symmetry, $S(G) = 0$ and the symmetry measure increases as it departs from G-symmetry, reaching maximal value (not necessarily 100). The maximal value of 100 is obtained if, e.g., one wishes to find the degree of pentagonality of a hexagon: the nearest pentagon to a hexagon is the collapsed pentagon into a single center point, the distance of which is, by definition, 100. All $S(G)$ values, regardless of G or of the structure, are on the same scale and therefore comparable. One can compare the degree of, say, perfect tetrahedricity (T_d-ness) and square planarity (the degree of D_{4h}-ness) of various distorted four-ligands molecules;[49] one can compare the D_{4h}-ness of molecules with different number of ligands; or one can compare different symmetry contents of different molecules. The main computational problem has been to find the nearest structure that has the desired symmetry, namely how to minimize eq 1 in order to get $\{P_k, k = 1,2...N\}$. Several methods, both general and problem-specific, have been constructed toward this goal, and are described in refs 17 and 30. For the evaluation of the level of tetrahedral distortion, $S(T_d)$, we use in this report the method of ref 30, and for evaluation of rotational symmetry content, $S(C_n)$, we use the method described in ref 50. As mentioned above, an important feature of the CSM approach is that it provides the actual shape of the nearest, searched symmetric object, i.e., the structure of the set of $\{P_i\}$.

II. Degree of Chirality. Evaluating the chirality content, S_{ch}, of an object by the CCM approach is based on the determination of the degree of the nearest achiral symmetry point group content.[29] This means searching for the minimal distance that the vertexes of the object have to undergo in order to attain achirality. The nearest achiral structure may have one reflection plane, and in this case $S(G_{achiral}) = S_{ch} = S(C_s)$, i.e., the nearest achiral point group is composed of the reflection and identity elements. A relevant example for this report is the helix: the nearest achiral structure to a helix is a plane onto which the helix points have been collapsed.[39] Another relevant example is the case of a chirally distorted tetrahedron, where the nearest achiral structure may be, e.g., of C_{2v} symmetry. The nearest achiral structure may even contain more than one mirror plane.[51,52] The achirality of the nearest structure need not be based on a mirror plane, but may have its origin in other improper symmetry elements such as inversion[34,53] or any S_n (n, an even integer). In practice, for the evaluation of the CCM, $S(G)$ is evaluated for every (relevant) $G_{achiral}$ and the minimal value is chosen; however, very often, $S_{ch} = S(C_s)$. Finally, $S(C_s)$ can never reach the maximal value of 100, because the distance to a nearest mirror plane is always smaller than the distance to a center point (see ref 29 for an explanation).

III. Specific Symmetry and Specific Chirality. In the context of the extension of the CSM and CCM approaches from molecules to materials, we define an additional symmetry measure, the *specific symmetry measure*, $S^*(G)$, and its special case of *specific chirality measure*, S^*_{ch}. The need for that additional measure

(30) Pinsky, M.; Avnir, D. *Inorg. Chem.* **1998**, *37*, 5575.
(31) Alvarez, S.; Llunell, M. *J. Chem. Soc., Dalton Trans.* **2000**, 3288.
(32) Pinsky, M.; Lipkowitz, K. B.; Avnir, D. *J. Math. Chem.* **2001**, *30*, 109.
(33) Katzenelson, O.; Zabrodsky Hel-Or, H.; Avnir, D. *Chem. Eur. J.* **1996**, *2*, 174.
(34) Buch, V.; Gershgoren, E.; Zabrodsky Hel-Or, H.; Avnir, D. *Chem. Phys. Lett.* **1995**, *247*, 149.
(35) Katzenelson, O.; Avnir, D. *Chem. Eur. J.* **2000**, *6*, 1346.
(36) Keinan, S.; Avnir, D. *J. Am. Chem. Soc.* **2000**, *122*, 4378.
(37) Keinan, S.; Avnir, D. *J. Am. Chem. Soc.* **1998**, *120*, 6152.
(38) Keinan, S.; Avnir, D. *J. Chem. Soc., Dalton Trans.* **2001**, 941.
(39) Katzenelson, O.; Edelstein, J.; Avnir, D. *Tetrahedron: Asymmetry* **2000**, *11*, 2695.
(40) Aullon, G.; Lledos, A.; Alvarez, S. *Angew. Chem., Int. Ed.* **2002**, *41*, 1956.
(41) Brancato, G.; Zerbetto, F. *J. Phys. Chem. A* **2000**, *104*, 11439.
(42) Lipkowitz, K. B.; Schefzick, S. *Chirality* **2002**, *14*, 677.
(43) Pettjean, M. *CR Acad. Sci. II C* **2001**, *4*, 331.
(44) Kohl, P. B.; Patrick, D. L. *J. Phys. Chem. B* **2001**, *105*, 8203.
(45) Alikhanidi, S.; Kuz'min, V. *J. Mol. Model* **2001**, *7*, 143.
(46) Jonas, J. *Chem. Listy* **2001**, *95*, 342.
(47) Aires-de-Sousa, J.; Gasteiger, J. *J. Chem. Inf. Comput. Sci.* **2001**, *41*, 369.
(48) Benigni, R.; Cotta-Ramusino, M.; Gallo, G.; Giorgi, F.; Giuliani, A.; Vari, M. R. *J. Med. Chem.* **2000**, *43*, 3699.
(49) Keinan, S.; Avnir, D. *Inorg. Chem.* **2001**, *40*, 318.
(50) Salomon, Y.; Avnir, D. *J. Comput. Chem.* **1999**, *20*, 772.
(51) Alvarez, S.; Pinsky, M.; Avnir, D. *Eur. J. Inorg. Chem.* **2001**, 1499.
(52) Alvarez, S.; Pinsky, M.; Llunell, M.; Avnir, D. *Cryst. Eng.* **2001**, *4*, 179.
(53) Kanis, D. R.; Wong, J. S.; Marks, T. J.; Ratner, M. A.; Zabrodsky, H.; Keinan, S.; Avnir, D. *J. Phys. Chem.* **1995**, *99*, 11061.

arises from the size-normalized $S(G)$ through its division by the sum of the squared distances (eq 1). Although this normalization is useful and needed for the comparison of different molecules and building blocks, consider the situation of a macromolecule composed of repeating units, such as the helix of quartz. Then, while the $\Sigma|Q_k - P_k|^2$ term in eq 1 for each of the units along the helix (say, the k vertexes that form one turn) is the same, the distance of each Q_k to Q_0 increases along the helix. In such cases the denominator increases faster than the nominator and $S(G)$ decreases with size, blurring the fact that there is a constant value to the repeated unit. Hence, there is also use for a symmetry measure which is not size normalized, namely

$$S^*(G) = S(G) \times D^2 = 100 \times \min \frac{1}{N} \sum_{k=1}^{N} |Q_k - P_k|^2 \quad (2)$$

$S^*(G)$ is a density-like (or specific) structural property. Because the number of atoms in a unit length of the helix is constant, division of $\Sigma|Q_k - P_k|^2$ by N is equivalent to the division by the total helix length, and one expects it to reach a constant value, which is characteristic of the bulk as a whole. Thus, whereas we shall use S_{ch} to address questions such as the chirality of the second shell tetrahedron, $SiSi_4$, S^*_{ch} will be used for answering a question such as, what is the chirality of quartz as a whole, along the helix axis?

3. Results and Interpretations: Structural Analyses

3.1. Symmetry and Chirality Analyses of the Elementary Building Blocks of Quartz. For the analysis of the symmetry and chirality of quartz we selected three characteristic units: the basic tetrahedron SiO_4 (which we shall call the first tetrahedron), the second-nearest tetrahedron $SiSi_4$ (the second tetrahedron), and the $Si(OSi)_4$ unit. The helices of quartz are investigated in the next section (3.2).

SiO_4 in quartz is not a perfect tetrahedron. A typical specific example[54] was found to be characterized by two pairs of bonds of different lengths, 1.608 and 1.609 Å, by two angles of 108.7°, two other angles of 110.5°, one angle of 108.8°, and one of 109.5°. On our symmetry scale the degree of tetrahedricity of this unit is $S(T_d) = 0.0094$. This deviation value from tetrahedricity is small, but, as we shall see below, significant. It should be noted that in many structural studies of quartz and other silicates, an assumption is made that SiO_4 is a perfect tetrahedron;[16] we stress that this is not the case and that the imperfection in this elementary building block is amplified in larger units. Indeed, the tetrahedral distortion of the second tetrahedron ($SiSi_4$) is more pronounced with $S(T_d) = 4.652$.

Once established as imperfect tetrahedra, the deviations of SiO_4 and $SiSi_4$ from tetrahedricity can be such that some of the reflection mirrors are retained (e.g., a distortion leading from T_d to C_{2v}), or such that remove all of the reflection mirrors. The latter case is special because if this type of distortion occurs, it leads to chirality of the building blocks. And, indeed, it turns out that in quartz, both the first and the second tetrahedra contain no mirror planes; both are therefore chiral. Interestingly, the chirality is not due to a drop in symmetry from T_d to C_1; a C_2-rotation axis is retained in both tetrahedra. The degree of chirality of SiO_4 [54] is $S_{ch} = 0.0007$, which is very small; and that of $SiSi_4$ is $S_{ch} = 0.555$. We see that the second tetrahedron is more T_d- distorted and also more chiral. (This need not always be the case: a tetrahedron, as explained above, can be distorted into one of the achiral T_d-subgroups). The CCM methodology also identifies the nearest achiral structure, which for SiO_4 and for $SiSi_4$ is a C_{2v} tetrahedron.

Chirality analysis is also applicable to the full unit of $Si(OSi)_4$, which is not a distorted T_d, but a distorted $\mathbf{S}_4$ symmetry (the symmetry of an improper rotation axis of order 4)-building block. Being an achiral point group, $S(\mathbf{S}_4) = S_{ch}$ and the specific value for $Si(OSi)_4$ is 0.743, with the nearest achiral object being a perfect $\mathbf{S}_4$.[55] It is the easy compressibility of the SiOSi angle within this building block[57] that enables the rich library of the many different types of silicates.

Finally, going to various quartz sources and origins, it is interesting to see the level of variability in the tetrahedricity and chirality values, if such exists at all. Variability was indeed detected, and typical examples[8,9,14,15,54,58−65] are collected in Figure 2.

3.2. Symmetry and Chirality of the Helices of Quartz. *I. Helical Structure and Its Relation to the Tetrahedral Unit.* It was first suggested by Fresnel that the structural dissymmetry of a uniaxial crystal such as quartz is due to a helical arrangement of the atoms.[66] Indeed, the most representative molecular feature of quartz is that the silicon atoms, the oxygen atoms, and various possible units composed of these atoms, are arranged in a variety of helical laces. In particular, literature has focused on the helices, which are composed of SiO_4 tetrahedra linked through a shared oxygen atom (Figure 1). Several types of SiO_4 helices can be identified within quartz, depending on the angle of view.[67] For instance, a common viewing angle of the structure of quartz is through the **c** axis (the optical

(54) Will, G.; Bellotto, M.; Parrish, W.; Hart, M. *J. Appl. Crystallogr.* **1988**, *21*, 182.

(55) One may ask a question which, to the best of our knowledge, has not been asked before: What is a left-handed chiral SiO_4 tetrahedron, and what is a right-handed one? And likewise, what are the handednesses of the $SiSi_4$ and $Si(OSi)_4$ units? This novel question deserves full attention by its own right, and we shall devote a separate full report to this issue. In the meantime the interested reader is referred to a recent report in which we analyzed the inherent difficulty of attaching right/left labels to chiral objects (particularly helices);[56] quartz is no exception from this point of view.

(56) Pinto, Y.; Avnir, D. *Enantiomer* **2001**, *6*, 211.

(57) Hazen, R. M.; Finger, L. W. *Sci. Am.* **1985**, *252* (5), 84.

(58) Le Page, Y.; Donnay, G. *Acta Crystallogr.* **1976**, *B32*, 2456.

(59) Zachariasen, W. H.; Plettinger, H. A. *Acta Crystallogr.* **1965**, *18*, 710.

(60) Levien, L.; Prewitt, C. T.; Weidner, D. J. *Am. Mineral.* **1980**, *65*, 920.

(61) Jorgensen, J. D. *J. Appl. Phys.* **1978**, *49* (11), 5473.

(62) Hazen, R. M.; Finger, L. W.; Hemley, R. J.; Mao, H. K. *Solid State Commun.* **1989**, *72*, 507.

(63) Chelikowsky, J. R.; Binggeli, N.; Keskar, N. R. *J. Alloys Compd.* **1993**, *197*, 137.

(64) Glinnemann, J.; King, H. E., Jr.; Schulz, H.; Hahn, Th.; LaPlaca, S. J.; Dacol, F. *Z. Kristallogr.* **1992**, *198*, 177.

(65) Kihara, K. *Eur. J. Mineral.* **1990**, *2*, 63.

(66) Lowry, T. M. *Optical Rotatory Power*; Dover Publications: New York, 1964.

(67) Glazer, A. M.; Stadnicka, K. *J. Appl. Crystallogr.* **1986**, *19*, 108.

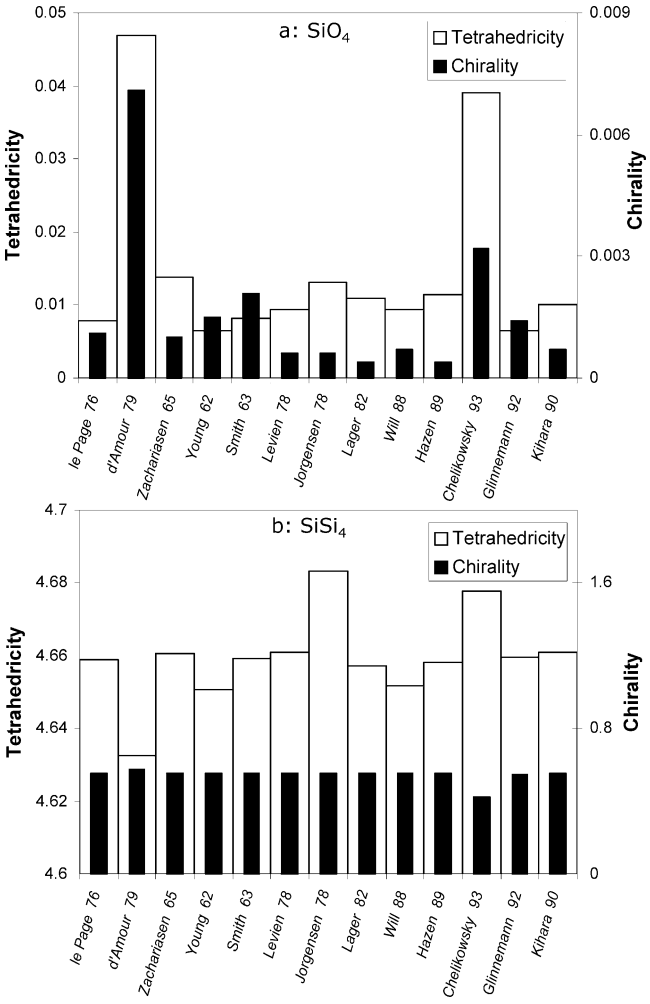

Figure 2. Variability in the degree of the tetrahedricity and the chirality values for the first tetrahedron, SiO_4 (a), and for the second tetrahedron, $SiSi_4$ (b), as obtained from x-ray data on quartz from various sources.[8,9,14,15,54,58−65]

axis), i.e., along the screw axis of the unit cell (Figure 1, top), where one can identify two types of helices.[68] One helix is composed of three SiO_4 tetrahedra per turn (which we call the H-3 helix). This helix is used as the crystallographic screw axis label for quartz, 3_2, with 3_1 as its enantiomeric helix (Figure 1, right), i.e., the crystallographic chiral space group labels of quartz are $P3_221$ for the right-handed helix and $P3_121$ for its enantiomer. Another helical structure that can be identified along the **c** axis is composed of paired helices of the same handedness (as in DNA's double helix) with six tetrahedra per turn (which we call the H-6 helices, Figure 1, left). Interestingly, the H-3 and the H-6 helices are of *opposite* handedness. Despite these opposite helicities, the crystal as a whole is chiral. If helices within a structure are the same but with opposite handedness forming an internal racemic structure, then the crystal as a whole will be achiral. In quartz, however, the opposite handedness retains the overall chirality because the opposing helices are different.

An important question regards the possible connection between the chirality of the SiO_4 building block and the chiral helical structure: Does the chirality of the small building block trigger the helix formation, or is it the chirality of the helix that imposes distortion of the SiO_4 tetrahedron? We propose that the latter reflects the situation for quartz. It should be noted first that for a general helical graph, not only is it chiral as a whole, but any portion of it − an arc of any length − must be chiral as well. However, in the physical world, there is a lower limit of building blocks of finite size, and even if they are achiral (atoms, pixels[33]) they still can be connected in the form of a helix. In this case, the minimal chiral unit − the shortest arc − will be a segment of four building blocks (because one, two, and three building blocks are the achiral point, line, and plane, respectively). So it seems that, a priori, one could build a helix from Si and O atoms, leaving the structural burden on the Si−O−Si bond. Indeed, torsions, which are based on large amplitude vibrations,[69] require only small forces. But how should the fact that each of the Si and O atoms is part of a helix affect the tetrahedral symmetry? Smith showed,[70] based on symmetry considerations and unit-cell data, that the SiO_4 tetrahedron (in both high and low quartz) *must* be slightly distorted. The possibility exists that the small chirality of the first tetrahedral building block of quartz is inherent (in the gas phase) and therefore dictates the chirality of the whole (as in the numerous reports of linear polymers which easily fold into helices by only minute chiral disturbances [71]). But, to the best of our knowledge, there is no proof that this is the case for quartz. In this context we mention that Hargittai et al.[72] observed flattening of the $\mathbf{S_4}$ symmetry of gas-phase $Si(OMe)_4$. However, although symmetry analysis of the SiO_4 core in this molecule resulted in $S(T_d) = 0.2379$, the unit as a whole is C_{2v}-achiral.

The hundreds of known SiO_4-based silicates and zeolites (all of which are based on the SiO_4 unit) point to the other possibility, namely that the helix is an energetic (local) minimum structure (as evident, in fact, by the very existence of quartz in nature), and that it is this long-range structure that imposes chirality on its own building blocks. Thus, in the rich map of silicate energy minima which are due to long-range structures, each of these structures "pays" by distorting its SiO_4 unit in a unique way. Helical SiO_4 are found not only in quartz but in other silicates as well,[73] and we mention that there is growing evidence for helical SiO_4-based structures even in disordered silica sol−gel materials.[74,75] Finally, it may be more than a coincidence that the C_2 symmetry which is characteristic of a perfect helix, is also the symmetry of the distorted SiO_4 unit. As mentioned above, the force required for the torsion of a linear chain into a helix is weak,[69] but then the accumulated force of the chain as a whole is enough to

(68) Heaney, P. J. *Rev. Mineral.* **1994**, *29*, 1.
(69) Rankin, D. W. H. In *Structures and Conformations of Non-Rigid Molecules*; Laane, J., Dakkouri, M., van der Veken, B., Oberhammer, H., Eds.; Kluwer Publishing: Amsterdam, 1993; p 519.
(70) Smith, G. S. *Acta Crystallogr.* **1963**, *16*, 542.
(71) Li, C. Y.; Cheng, S. Z. D.; Weng, X.; Ge, J. J.; Bai, F.; Zhang, J. Z.; Calhoum, B. H.; Harris, F. W.; Chien, L.-C.; Lotz, B. *J. Am. Chem. Soc.* **2001**, *123* (10), 2462.
(72) Boonstra, L. H.; Mijlhoff, F. C.; Renes, G.; Spelbos, A.; Hargittai, I. *J. Mol. Struct.* **1975**, *28*, 129.
(73) Peacor, D. R. *Z. Kristallogr.* **1973**, *138*, 274.
(74) Jung, J. H.; Ono, Y.; Hanabusa, K.; Shinkai, S. *J. Am. Chem. Soc.* **2000**, *122*, 5008.
(75) Yang, S. M.; Sokolov, I.; Coombs, N.; Kresge, C. T.; Ozin, G. A. *Adv. Mater.* **1999**, *11*, 1427.

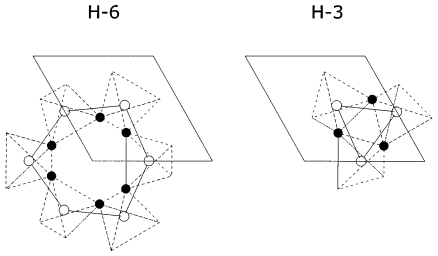

Figure 3. Six types of helices within quartz analyzed in this report (shown at the same projection of Figure 1, top): helices of SiO_4 tetrahedra (dotted lines) of H-3 and of H-6; the helices formed by the skeleton of silicon atoms (H-3(Si) and H-6(Si), open circles); and the helices of the *inner* oxygen atoms (H-3(O) and H-6(O), black circles).

show up in the slight helical torsion of the tetrahedral building block.

II. Helicity, Symmetry, and Chirality of Quartz Helices. Following the general comments on the helicity, we now move to the quantitative evaluation of its symmetry and chirality. The helix we analyze is the general $(SiO_4)_n$ helix, where we sweep over n. To evaluate the degree of helicity within quartz, one must define the reference "ideal" helical shape. There are many ways to define the ideality of a helix: it may be conical, cylindrical, with polygonal top projection, with regular pitch or an oscillating one, and so on. We evaluated the degree of the helicity of finite-size helix-segments by probing two symmetry elements which are of relevance to the quartz helices: the C_2-symmetry (with the C_2 axis bisecting the long helical axis), which represents an ideal cylindrical helix; and the C_3 symmetry of the top projection (Figure 1), which represents the $P3_221$ space group. Perfect helicity is then characterized then by zero values for $S(C_2)$ and $S(C_3)$.

Six types of helices within quartz were examined (Figure 3): the H-3 helix of SiO_4 tetrahedra; the helix formed by the skeleton of silicon atoms (H-3(Si)); the helix of the *inner* oxygen atoms (the oxygen atoms that form the inner "hole", H-3(O)); one of the two H-6 tetrahedral helices (Figure 1); and its corresponding H-6(Si) and H-6(O) helices.

H-3 Helices. The $S(C_3)$ value of the projection of all three H-3 helices is zero, representing the $P3_221$ space group, and so is the $S(C_2)$ of the Si atoms helix, H-3(Si), and of the O atoms helix, H-3(O) (Figure 4a). Thus, *the helicities of the Si skeleton and of the O skeleton are perfect*. Not so for the $S(C_2)$ of the full tetrahedra (Figure 4a), in which the $S(C_2)$ the value rises steeply to a maximum at three tetrahedra, and then gradually decreases. The perfect C_2 symmetry of the skeletons helix (Si and O) is lost in the full tetrahedral helical structure, already at the fragment of two tetrahedra (despite the fact that each tetrahedron is C_2 symmetric). Following the maximum, the $S(C_2)$ value decreases gradually because of the size normalization of the symmetry measure. To understand it intuitively imagine an extremely ("infinitely") long helix, squeezed into a unit size; then the helical angle approaches zero, and one has a helix which is almost a stack of parallel rings. The C_2-symmetry of such a stack is perfect, and therefore $S(C_2)$ approaches zero.

The perfectly C_2-symmetric H-3(O) and H-3(Si) helices are, of course, chiral, but so is a helix which deviates

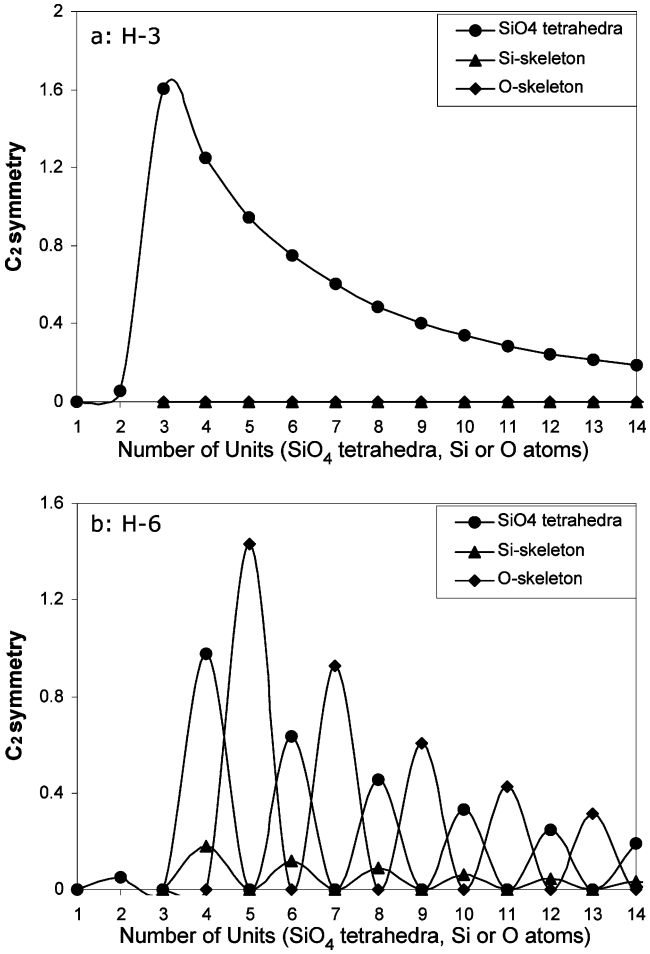

Figure 4. Changes in the degree of C_2 symmetry of the six types of helices (Figure 3) in low-quartz: (a) H-3 helices; (b) H-6 helices.

from this symmetry, namely the full H-3 helix, as shown in Figure 5a. Note that the chirality of the helices is much higher than the chirality of the three molecular building blocks analyzed in Section 3.1. Because the chirality of H-3(O) and H-3(Si) is due solely to its perfect helicity, understanding its behavior will serve as a reference to the understanding of the other helices. It is seen that the two helices behave similarly (Figure 5a). As explained above, after the first three atoms, all of which are achiral (a point, a line, and a plane, respectively), the fourth atom forms the smallest chiral helix segment. Interestingly, this segment is also *the most chiral* one. From this point and on, the chirality falls down gradually with size, as we have seen for $S(C_2)$, and for a similar reason given for the $S(C_2)$ behavior: a helix which is practically a stack of parallel rings is achiral.

We note that the chirality of the Si helix is higher than the chirality of the O helix. This is due to the fact that the radius of the O helix is smaller than the radius of the Si helix. To understand why reducing the radius of a helix decreases its chirality, consider again a helix which is infinitely thin and therefore achiral. The tetrahedral helix, H-3, follows an overall similar trend, but it is clerically seen that an oscillatory behavior is superimposed on it every fourth tetrahedron, namely after every $^4/_3$ turns. In fact, after rising from almost zero for the first tetrahedron, the most chiral segment

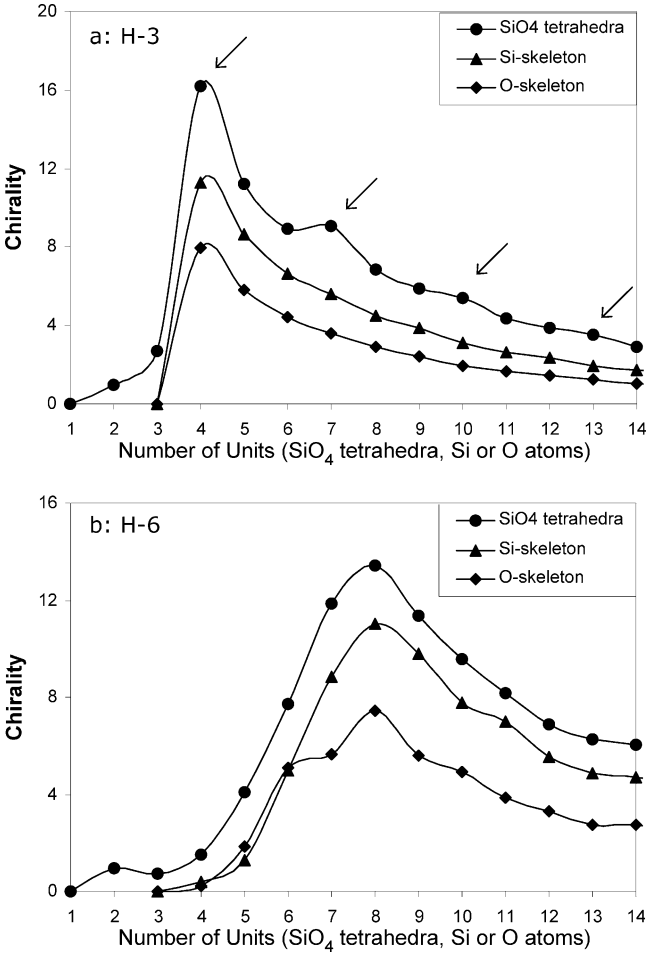

Figure 5. Changes in the degree of chirality of the six types of helices in low-quartz: (a) H-3 helices; (b) H-6 helices. Arrows indicate the oscillations.

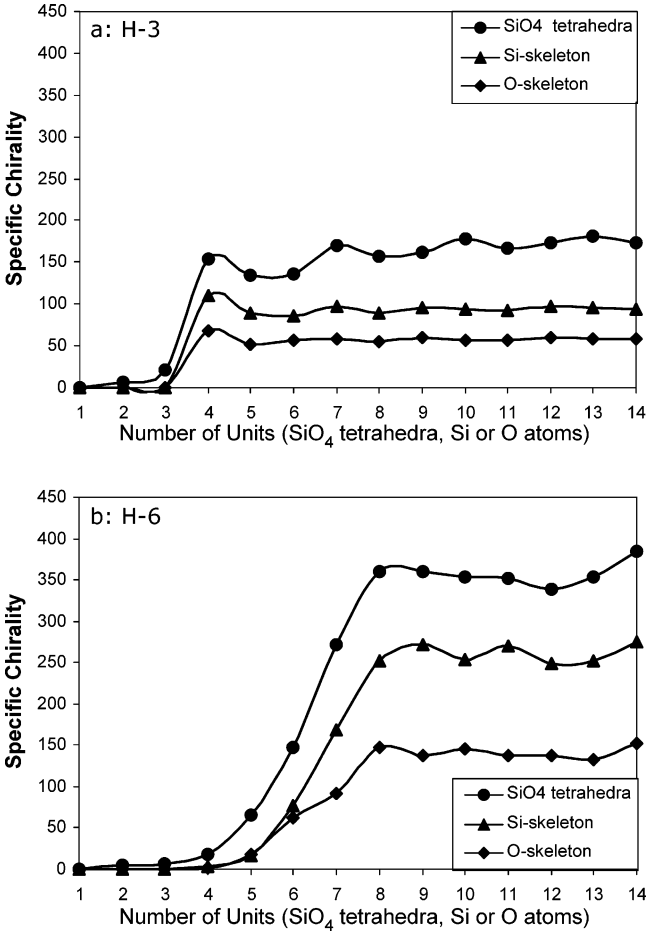

Figure 6. Evolution of the specific chirality, S^*_{ch}, of the six types of helices in low-quartz: (a) H-3 helices; (b) H-6 helices.

is obtained, namely the first four-tetrahedron segment (Figure 5a), and this peak repeats itself with diminishing power every four tetrahedra. Elsewhere we analyzed the behavior of helices and of a mathematical helix[39] and showed that the oscillatory superposition (more weakly recognizable in the Si and O skeleton helices) is an inherent property of this structure.

H-6 Helices. As for the H-3 helices, the $S(C_3)$ values of the projections of the three H-6 helices (the Si helix, the O helix, and the tetrahedral helix) are zero, again representing the $P3_221$ space group. Interestingly, the $S(C_2)$ of the H-6 helices (Figure 4b) behaves completely differently than the $S(C_2)$ of the H-3 helices (Figure 4a): pronounced oscillations in the symmetry values appear, and all three H-6 helices oscillate in their $S(C_2)$ values between perfect and gradually decreasing imperfect C_2 symmetry. For the full H-6 helix and for the H-6(Si) helix the $S(C_2)$ is zero at every odd unit, whereas for the H-6(O) it is zero at every even unit. The lack of C_2 symmetry in every even or odd unit can be understood by considering the **c**-axis projections of the helices (Figure 3) as reflecting the properties of the $P3_221$ space group. Thus, these projections show that although for the oxygens the C_3-symmetry is due to a hexagon whose bond lengths change alternatively while keeping the angles at 120°, for the silicons helix the C_3-symmetry is obtained by keeping the bond length of a perfect hexagon fixed while alternating the projected bond angles (between 108.3° and 131.7°). Thus, as demonstrated in Figure 3, for the oxygens helix projection, there is a C_2 axis, whenever there is an even number of atoms, which passes through the bond linking two neighboring atoms of the segment. For the silicons, the alternating angles of the projection dictate that the C_2 axis must pass through an Si atom, leaving to its left and to its right the same number of atoms; hence the shift in the behavior of the two helices. The full tetrahedra-helix behavior resembles that of the silicons helix because the Si atoms are located at the centers of the tetrahedra and therefore represent their location. To visualize this, consider three linked tetrahedra. The center tetrahedron is C_2-symmetric (see above) and so the axis of the triad must pass through it. As for chirality, the H-6 helices behave in a manner similar to that of the H-3 helices (Figure 5b). The maximum chirality value is again after $^4/_3$ turns, but this time it takes 8 units to reach this segment length.

Once we have the symmetry and chirality values of the building blocks and of the helices, we move on to calculate the specific chirality, S^*_{ch}, of these units, namely the structural characteristics of quartz as a whole. It is shown (Figure 6) that, as expected, asymptotic values are reached, and in fact, they are reached quite fast. A small number of elementary units already carries the properties of the whole. Because of this observation, we have selected the 4-units helix segments of the H-3 helix of the full tetrahedra as the character-

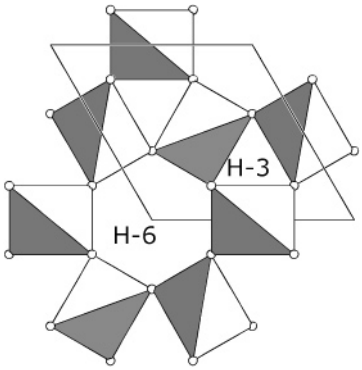

Figure 7. Structure of high quartz (viewed trough the **c** axis), $P6_222$, with its H-3 and H-6 helices.

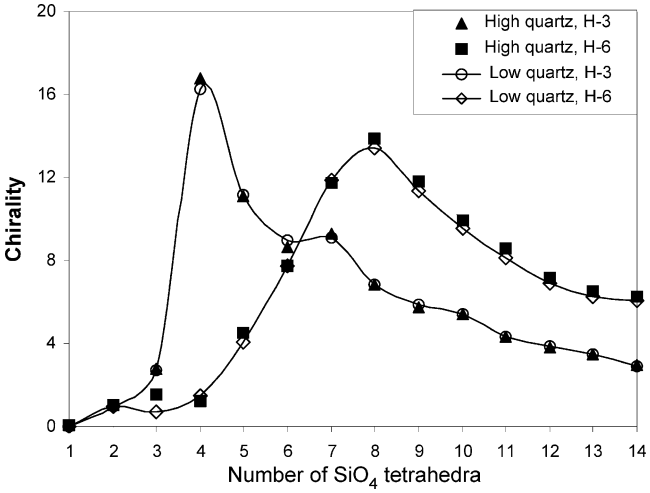

Figure 8. Degree of chirality of the H-3 and H-6 tetrahedral helices in low and high quartz.

istic chirality feature of quartz; hence we find that the specific chirality of quartz has a value of ~170.

3.3. Toward the Analysis of Related Materials: High Quartz and Cristobalite. *I. High Quartz.* The phase transition from low to high quartz, around 846 K, leads to higher space group symmetry, namely to $P6_222$ (or to the enantiomeric $P6_422$) (Figure 7, cf. Figure 1). The molecular motion leading to the space-group change is a small rotation of SiO_4 tetrahedra about the ⟨100⟩ direction.[68] Interestingly, the higher space group symmetry is not associated with a more perfect tetrahedricity of the SiO_4 unit.[76] It is $S(T_d) = 0.572$ compared with $S(T_d) = 0.0094$ for low quartz. By contrast, the second tetrahedron $SiSi_4$ distorts similarly in both types of quartz, with $S(T_d)$ values of 4.467 and 4.652, respectively. Another difference between high and low quartz is that that all high quartz helices (the Si, O, and SiO_4 H-3 and H-6 helices) are fully C_2-symmetric. On the other hand, as shown in Figure 8, the degree of chirality is kept almost unchanged upon the phase transition. Likewise, the specific chiralities, S_{ch}* are almost the same: for the tetrahedral H-3 helix it is 178 for high quartz, compared to 173 for low quartz.

II. Cristobalite. The methodology of symmetry and chirality analysis of crystalline materials developed and demonstrated in detail for quartz is general and applicable to other crystalline materials as well. Here we

(76) Wyckoff, R. W. G. *Z. Kristallogr.* **1926**, *63*, 507.

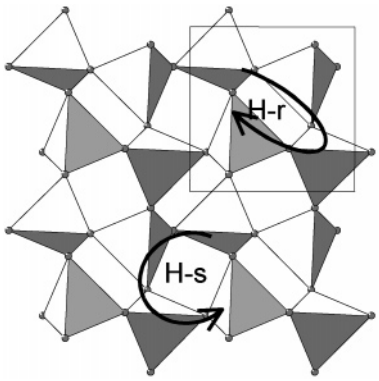

Figure 9. Structure of low cristobalite, $P4_121$, viewed along the **c** axis. The two helices, one with a rectangular projection (H−r) and the other with a square projection (H−s), are shown.

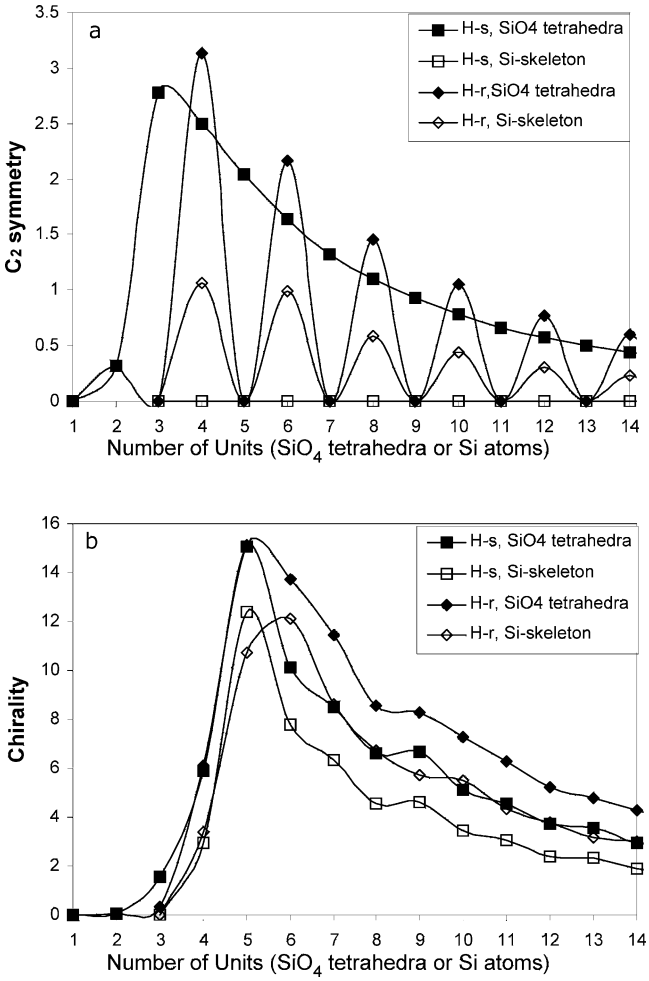

Figure 10. Variations in four types of helices of low-cristobalite crystal in the degree of (a) C_2 symmetry and (b) chirality.

demonstrate this generality by briefly commenting on another chiral SiO_2 material, low cristobalite[73] the space group of which is $P4_121$. As in quartz, here too the chirality is due to internal helicity, but with different details. In the cristobalite crystal one can identify two different helices along the **c** axis, as shown in Figure 9. One has a rectangular projection (the H−r helix) and the other has a square projection (the H−s helix). In Figure 10a we show some representative C_2-symmetry trends for this crystal, and it is seen that the behavior of H−r resembles that of H-3 of low quartz, whereas

the behavior of H−s resembles, with its oscillatory behavior, that of H-6 of low-quartz (Figure 4). The reasoning for the oscillations in both cases is the same. As for chirality (Figure 10b) it is interesting to note that, again, the maximal chirality value is obtained after one and a third turns of the helix (as in quartz), only that in this case more tetrahedra are needed for this number of turns, namely between 5 and 6. Finally, the specific chirality, S_{ch}* of cristobalite is ∼165 for the rectangular helix (similar to quartz).

4. Concluding Remarks

We have demonstrated the use of the concept of continuity in symmetry and chirality as a novel descriptor of the structure of the building blocks of materials. We emphasize the global nature of these measures which take into account all the angles and bond lengths. In this sense this is a new method in structure analysis studies which traditionally have concentrated on a selected, specific geometrical feature. We recall that for an *n*-vertexes structure there are $3n - 6$ degrees of freedom (9 for AB_4 structures), and therefore not taking all into account may amount to overlooking some important contributions to the overall distortion. Furthermore, if one wishes to compare different families of molecules or crystals, only global descriptors can be used. Changes in specific geometric descriptors will of course show up in the $S(G)$ values. The correlation between local and CSM descriptors was analyzed in detail by Alvarez and Llunell.[31]

The particular example we have selected for this study, quartz, was analyzed in depth. All of the important molecular building blocks were investigated, as were quartz' helices, and trends in their variation with size have been revealed and explained. It has become possible now to write a sentence such as "the specific geometric chiralities of low and high quartz are 170 and 180, respectively" and compare it to the cristobalite values of 165.

The next step then is to identify possible correlations between external parameters that affect the structure of materials, such as pressure and temperature, and symmetry and chirality; and possible correlations between symmetry and chirality and physical properties such as optical rotation; these, in the context of quartz, are the topics of our next reports.

Programs Availability. Scholars wishing to use the symmetry and chirality measurement programs are welcome to approach the authors.

Acknowledgment. We thank Dr. Mark Pinsky for close computational support, and Prof. Kenny Lipkowitz for detailed discussions on chirality measures. This project is supported by the U.S.−Israel Binational Science Foundation (Project 1998077) and by the Israel Science Foundation (Grant 30/01).

CM0207806